Bioinspired conductive cellulose liquid-crystal hydrogels as multifunctional electrical skins

Zhuohao Zhang[a,b,c], Zhuoyue Chen[c], Yu Wang[c], and Yuanjin Zhao[a,b,c,1]

[a]Department of Rheumatology and Immunology, The Affiliated Drum Tower Hospital of Nanjing University Medical School, 210008 Nanjing, China; [b]Department of Clinical Laboratory, Nanjing Drum Tower Hospital, Clinical College of Xuzhou Medical University, 210008 Nanjing, China; and [c]State Key Laboratory of Bioelectronics, School of Biological Science and Medical Engineering, Southeast University, 210096 Nanjing, China

Edited by David A. Weitz, Harvard University, Cambridge, MA, and approved June 22, 2020 (received for review April 13, 2020)

Bionic electronic skin (E-skin) that could convert external physical or mechanical stimuli into output signals has a wide range of applications including wearable devices, artificial prostheses, software robots, etc. Here, we present a chameleon-inspired multifunctional E-skin based on hydroxypropyl cellulose (HPC), Poly(Acrylamide--co-Acrylic acid) (PACA), and carbon nanotubes (CNTs) composited liquid-crystal hydrogel. We found that the HPC could still form cholesteric liquid-crystal photonic structures with the CNTs additive for enhancing their color saturation and PACA polymerization for locating their assembled periodic structures. As the composite hydrogel containing HPC elements and the PACA scaffold responds to different stimuli, such as temperature variations, mechanical pressure, and tension, it could correspondingly change its volume or internal nanostructure and report these as visible color switches. In addition, due to the additive of CNTs, the composite hydrogel could also output these stimuli as electrical resistance signals. Thus, the hydrogel E-skins had the ability of quantitatively feeding back external stimuli through electrical resistance as well as visually mapping the stimulating sites by color variation. This dual-signal sensing provides the ability of visible-user interaction as well as antiinterference, endowing the multifunctional E-skin with great application prospects.

bioinspired | cellulose | liquid crystal | electrical skin | carbon nanotube

Skin is the physical barrier between the human body and the external environment. It can convert external stimuli such as temperature, pressure, tension, and twisting force into electrical signals, which would be received by the brain for generating safe and effective instructions. Due to its being highly applicable to the fields of alternative prosthetics, intelligent robots, wearable devices, and medical diagnostics, this multisensory feature has prompted researchers to develop artificial flexible electrical skins (E-skins) with similar sensibilities (1–4). Many E-skins that could reflect external stimulus signals have been rapidly developed by integrating different conductive agents such as metals, alloys, liquid metals, ionic liquids, semiconductors, and carbon materials (5–10). Among these conductive agents, carbon nanotubes (CNTs) have been widely utilized because of their brilliant conductivity, diathermancy, and mechanical properties (11–13). However, most of the CNT integrated flexible E-skins lack data visualization, which requires connection of electrical instruments to process and display electrical signals. In addition, the single electrical signal output of these devices makes it difficult to locate the stimulation site and is easy to cause error under interference. Thus, the creation of conductive E-skin with additional visible signal output and displaying capabilities to locate stimulation is still anticipated.

In this paper, inspired by chameleons, we proposed a multifunctional E-skin by using a composite conductive cellulose liquid-crystal hydrogel, as shown in Fig. 1. Contrasting to human skin, chameleon's skin possesses additional capability to change its color by control inside periodic guanine nanocrystal arrays (14). In order to mimic this characteristic, intelligent structural color hydrogels, constructed by imparting the intelligent responsive polymers with periodical nanostructures which could modulate light propagation, have been developed (15–26). In particular, when combining cellulose liquid crystal with intelligent hydrogel scaffolds, the resultant composite hydrogel could generate structural colors in specific cellulose concentration and these colors would change under external stimulus due to the nanostructure variation (27–39). In addition, since it is derived from nature, cellulose has a great value of research due to its cheapness, biodegradability, and biocompatibility (40–42). With these attractive features, however, due to the poor conductivity and high transmissivity of cellulose, the intelligent cellulose liquid-crystal hydrogels with expected conductivity and visualization that could be utilized in flexible electronics remain unexploited.

Herein, we fabricate the desired cellulose hydrogel for E-skin by integrating the advantages of hydroxypropyl cellulose (HPC), thermal-responsive Poly(Acrylamide-co-Acrylic acid) (PACA) (43–45), and CNTs. It was found that the HPC could still form photonic liquid-crystal structure and show bright structural color with these additives, while the CNTs could enhance the saturation of the structural color and the PACA could locate the HPC assembled structure after polymerization. Due to the sensitive responsibility of the HPC elements and the PACA scaffold, the composite hydrogel could change volume or internal nanostructure under different stimuli including temperature variations, mechanical pressure, and tension, and correspondingly report these as visible color switches. In addition, benefiting from the doping of the conductive CNTs, the resistance of the hydrogel that changes with internal nanostructures could also be output as electrical signals. Thus, it was demonstrated that the

Significance

We present an electronic skin (E-skin) based on hydroxypropyl cellulose composite hydrogel with stable cholesteric liquid-crystal structures and bright structural colors. Due to the utilization of the composite hydrogel with multiple responsiveness as a main building block, the E-skin can respond to pressure, tension, and temperature, and perform optical sensing of these external stimuli through color migration caused by internal structural changes. By adding carbon nanotubes, the composite hydrogel can simultaneously output these stimuli as electrical signals. Due to this dual-responsive mechanism under stimuli, the E-skin has great research value in health care and variable devices.

Author contributions: Y.Z. designed research; Z.Z., Z.C., and Y.W. performed research; Z.Z. analyzed data; Z.C. and Y.W. contributed to scientific discussion of the article; and Z.Z. and Y.Z. wrote the paper.

The authors declare no competing interest.

This article is a PNAS Direct Submission.

[1]To whom correspondence may be addressed. Email: yjzhao@seu.edu.cn.

This article contains supporting information online at https://www.pnas.org/lookup/suppl/doi:10.1073/pnas.2007032117/-/DCSupplemental.

First published July 16, 2020.

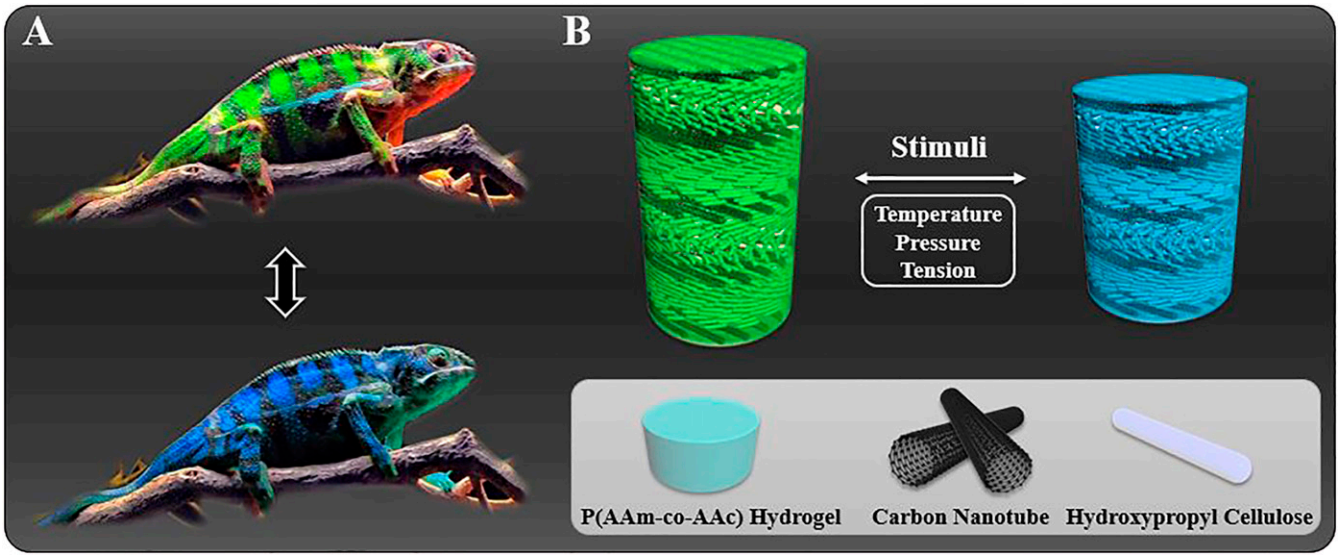

Fig. 1. Schemes of the conductive cellulose structural color hydrogel. (*A*) The color variation of the chameleon. (*B*) Schematic of the nanostructure and the composition of the conductive cellulose structural color hydrogel.

composite hydrogel composed E-skins could not only quantitively feedback multiple stimuli through electrical signals, but also visually report the location of the stimuli site via color changing. These features indicate that the conductive cellulose liquid-crystal hydrogel might open a chapter in designing and fabricating of multifunctional E-skin.

Results

In a typical experiment, the conductive cellulose structural color hydrogel was constructed by incorporating CNT, HPC, and PACA hydrogel. The pregel solution of PACA hydrogel was prepared and stored in a dark place. CNT and HPC with a certain concentration were added and dispersed in the pregel solution in batches for full dispersion. This mixture would self-assemble into cellulose nanocrystals in the dark. By pouring it into molds and polymerizing via ultraviolet (UV) light, the composited hydrogel with vivid color could be obtained. The formation of the striking structural color of the composite hydrogel is ascribed to the periodically arranged internal nanostructures. HPC, a derivation of cellulose, is soluble in water due to a large number of hydrogen bonds between its hydroxyl groups and water molecules. When the concentration reaches the range of 50 to 70 wt %, the HPC molecules in aqueous solution could form an anisotropic orderly arrangement under intermolecular forces such as molecular repulsion and form a lyotropic cholesteric mesophase. In this mesophase between liquid and crystal, HPC molecules are arranged in layers and the molecules in the layers are parallel to each other and parallel to the plane of the layer along the long axis. The arrangement direction of two adjacent molecular layers is slightly rotated, and these layers are periodically stacked into a spiral structure. The twist of this supermolecular structure is attributed to the chirality of the constituent molecules. When the molecular arrangement rotates 360° and returns to the original direction, the distance between the corresponding two layers where the molecular arrangement is exactly the same is called the pitch of the cholesteric liquid crystal (Fig. 2*A*). This periodic lamellar nanostructure could modulate the propagation of light in it, and the pitch corresponds to the wavelength of the scattered light. Through scanning electron microscopy (SEM), the periodically stacked nanostructure could be observed (Fig. 2 *B* and *C*). Typically, when the wavelength mentioned above is exactly in the wavelength range of visible light, these materials would be rendered the characteristics of optical coloration. Generally, the value of the reflection wavelength (λ) of the material could be estimated by the De Vries equation (46)

$$\lambda = \tilde{n}\, p\cos\theta, \qquad [1]$$

where $\tilde{n}$ refers to the average refractive index of the cholesteric liquid crystal, p is the helical pitch of the cholesteric phase, and θ is the angle between the incident light and the cholesteric helix axis. According to Eq. 1, the color of the composite hydrogel is regulated by the helical pitch. Thus, a series of hydrogels with striking structural colors could be fabricated by adjusting the concentration of HPC (*SI Appendix*, Fig. S1). As the HPC concentration increased from 50 to 70 wt %, the colors of the materials varied from red to blue (Fig. 2*D*). This fact could be ascribed to the reduction of the helical pitch of the cholesteric liquid crystal.

The structural color of the hydrogel provided E-skin with visual interaction, which was lacking in most of the existing materials. To further investigate this optical property, the corresponding characteristic reflection spectra of hydrogels were measured (Fig. 2*E*). It was found that the HPC concentration is linearly negative relative to the reflection peak of the spectrum (*SI Appendix*, Fig. S2). The combination of PACA hydrogel was to lock the nanocrystal within its network, but also imparted the material with reversibility for further sensing. In addition, the incorporation of hydrogels and CNTs would not affect the coloration ability of the HPC cholesteric liquid crystal. Attractively, the color saturation of such material even increased due to the dark background of CNTs (*SI Appendix*, Fig. S3). In addition to the improvement of optical properties, the introduction of CNT also endowed the composite hydrogel with good conductivity, which is positively correlated with the increase of CNT concentration.

In order to investigate the electrical properties of the composite conductive hydrogel, a series of hydrogels with different sizes was fabricated (*SI Appendix*, Fig. S4 *A* and *B*). The concentrations of HPC and CNTs were 68% and 2 wt %, respectively. The resistances of these materials were measured by a digital multimeter. According to the resistance (R) formula

$$R = \rho L/ab, \qquad [2]$$

ρ is the resistivity of the composite conductive hydrogel, L, a, and b are the length, width, and thickness of the material,

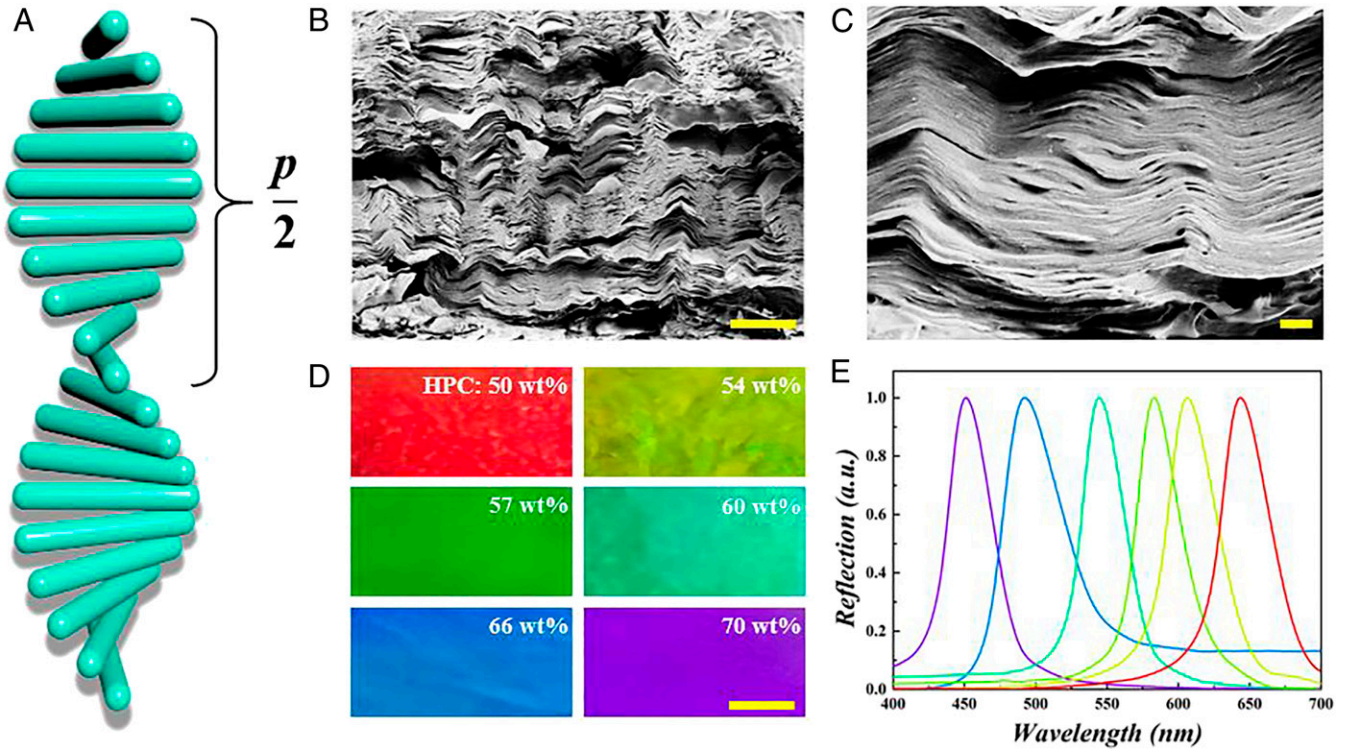

Fig. 2. The optical properties and the nanostructure of the conductive cellulose liquid-crystal hydrogel. (*A*) Schematic of HPC molecular nanostructure along the helix axis of cholesteric liquid crystal. (*B* and *C*) SEM images of the nanostructure of the hydrogel. (*D*) Optical images of conductive hydrogels with 2 wt % CNT and HPC with the concentration from 50 to 70 wt %. (*E*) The characteristic reflection spectra of the above hydrogels. (Scale bars: 20 μm in *B*, 2 μm in *C*, and 2 mm in *D*.)

respectively. Thus, the resistance of an E-skin is positively related to its length and negatively related to its width or thickness. The relationship between the length, width, and thickness of the material and its resistance was studied. The length of the material represents the length of the polydimethylsiloxane (PDMS) films rather than the distance of the two conductive tapes. It was found that when the width and thickness of the hydrogel are unified, the longer the material length, the higher its resistance, and they showed a nearly linear relationship (*SI Appendix*, Fig. S4*C*). Then, resistance tests were performed on materials of different widths and thicknesses. It was shown that when the other two parameters are fixed, the larger the width or thickness, the smaller the resistance of the material (*SI Appendix*, Fig. S4 *D* and *E*), which was consistent with theoretical results.

Compared to general structural color cellulose hydrogels, the composite hydrogel was sensitive to external temperature variation due to the thermal responsiveness of PACA. PACA hydrogel is formed by cross-linking a large amount of acrylamide and acrylic monomers. When the temperature rises, the intramolecular hydrogen bonds between acrylamide and acrylic acid break and they connect to the hydrogen bonds of the water molecules. Thus, the hydrogel absorbs water and expands in volume. Conversely, when the temperature decreases, the hydrogen bonds between polymer monomers and water molecules break, and intramolecular hydrogen bonds are reformed. Therefore, the hydrogel releases water molecules and shrinks in volume. Therefore, when this temperature-sensitive hydrogel is utilized as a scaffold for HPC and CNT, the composite hydrogel would be rendered with attractive optical, electrical, and thermal responsive properties. When the ambient temperature rises, the helical pitch of the HPC increases due to the expansion of the hydrogel scaffold, resulting in an increase in the wavelength of reflection and a shift in the visual color toward red. Therefore, these composite hydrogels could realize the perception of external temperature and reflect this change in real time through color changes. It should be mentioned that the structural color of the cholesteric liquid crystal would also respond to the change of temperature. This could be ascribed to the variation of the pitch of the HPC anisotropic layers under the change of intermolecular force. However, since this color change tendency was the same as the color shift caused by the hydrogel volume change, it would not affect the thermal sensing of the composite hydrogel and played a synergistic effect. The elasticity of the PACA scaffold also imparted the material with the ability of reversible recovery after being subjected to external stimuli. In addition, due to the change of nanostructure, the dispersity of internal CNTs would also change, which leads to the change of material resistance. Thus, by studying the relationship between temperature and the characteristic reflection peak as well as the resistance of the hydrogel, the real-time external temperature could be reported through optical and electrical signals.

These electrical and optical features encouraged us to use the conductive cellulose liquid-crystal hydrogels to design and fabricate functional E-skins with multistimulus responsiveness. To protect the hydrogels from mechanical wear, PDMS films were utilized in the following experiments. A palm-shaped E-skin was prepared for the thermal-sensitivity detection (Fig. 3*A*), which was composed of an HPC concentration of 50, 60, and 68 wt %, respectively, as well as a CNT concentration of 2 wt %. A digital camera recorded the color change process of the E-skin from 0 to 40 °C and then returned to 0 °C, and the characteristic reflection spectra were measured every 5 °C. It was found that as the temperature increased from 0 to 40 °C, the colors of the electronic skins all showed a redshift (Fig. 3*B*). The wavelengths of the characteristic reflection peaks of the three hydrogels gradually increased, and the average offset was about 3 nm/°C. In

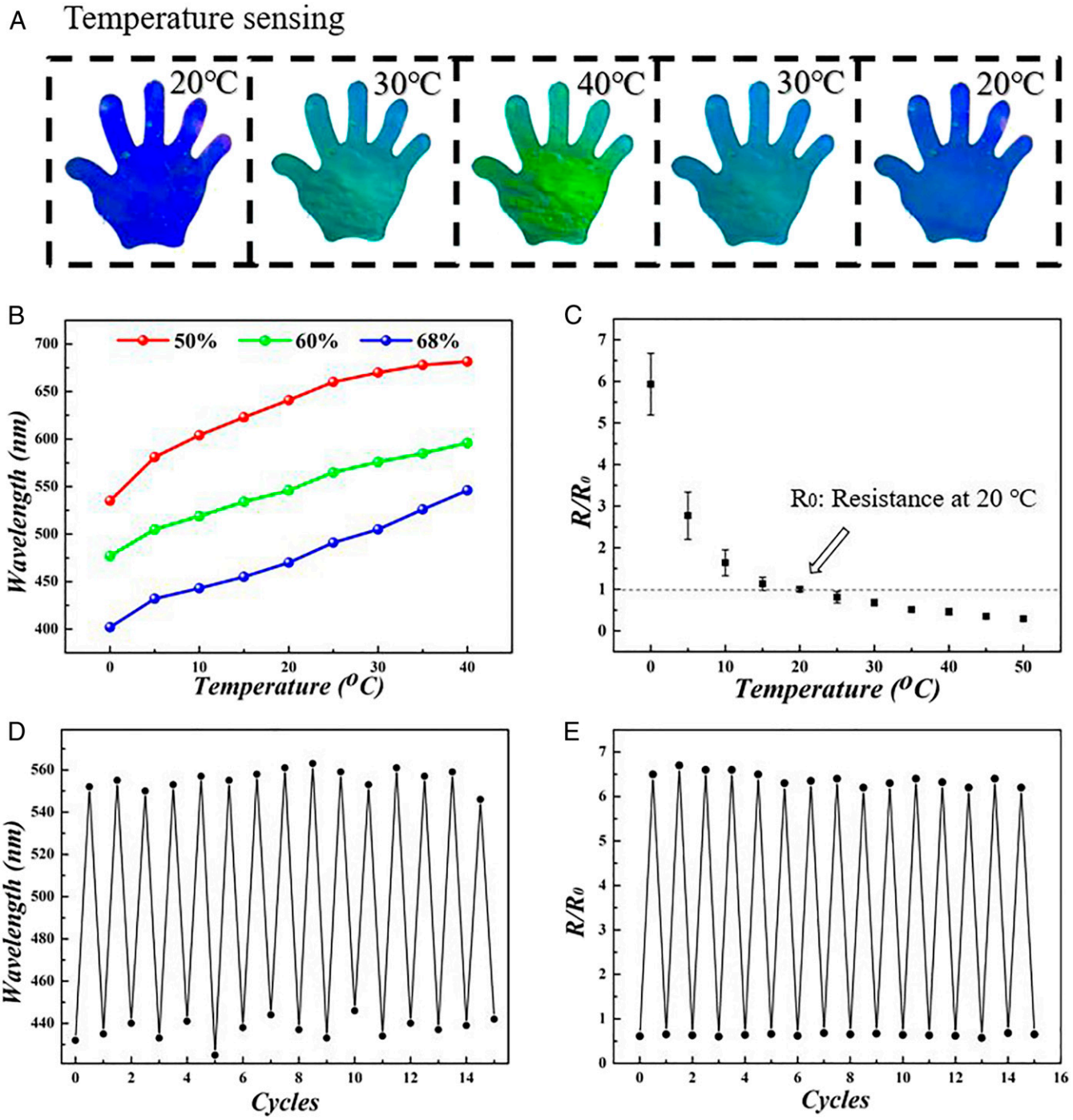

Fig. 3. The temperature sensing test of the E-skin. (*A*) Optical images of the color variation of a palm-shaped E-skin under temperature change. (*B*) The relationship between the wavelength of the E-skin and temperature; the HPC concentrations of these E-skins were 50, 60, and 68 wt %. (*C*) The relationship between relative resistance and temperature. The dotted line represents the R_0, which is the resistance of the E-skin at room temperature (20 °C). (*D*) The position of reflection peak of the E-skin with an HPC concentration of 65 wt % under cyclic tests of temperature. (*E*) The resistance of the E-skin with an HPC concentration of 65 wt % under cyclic tests of temperature.

addition to the visual signals, the resistances' variation during this process were also measured with a multimeter. As shown in Fig. 3*C*, the hydrogels expanded and the resistances of E-skin gradually decreased. The resistance at the preset room temperature of 20 °C was set as the standard value R_0. When the temperature dropped to 0 °C, the resistance increased to six times of R_0. While the temperature rose to 40 °C, the resistance decreased to 40% of the original. The cyclic experiments had verified the reversibility of the material's thermal–optical and thermal–electrical sensing responsiveness (Fig. 3 *D* and *E*). It was found that the thermal sensitivity of the material remained after heating and cooling cycles, and it could return to its original state after the stimulation was completed.

In addition to generating dual-signal output to external temperature, the E-skin could also respond to mechanical forces such as pressure and tension. When the conductive hydrogel in

the middle layer was deformed under forces, changes in the internal nanostructure of the composite hydrogel would lead to color shift and change in conductivity. The palm-shaped E-skin was also utilized in pressure sensing. By pressing the surface of the E-skin, it was found that a significant blueshift in color occurred in the stressed area (Fig. 4*A*). Gradient pressures were applied to the same position as the material, and its resistance and reflection peak wavelength were measured. It should be mentioned that the measurement area of the materials is fixed at the 2 mm × 2 mm area around the stimuli spot. It was found that the resistance of the E-skin would increase linearly with increasing pressure, while its reflection peak wavelength would decrease linearly during the process (Fig. 4 *B* and *C*). These electrical and optical properties would still be maintained after repeated cycling tests (*SI Appendix*, Fig. S5 *A* and *B*). In addition, rectangular E-skins were prepared for the evaluation of tensile sensibility, and the changes in tensile force were presented by the length of the E-skin being stretched (Fig. 4*D*). As the E-skin was gradually stretched, its color gradually shifted toward blue. The resistance linearly increased, and the wavelength of reflection peak also linearly decreased during this process (Fig. 4 *E* and *F*). Due to the excellent stretchability of both the PDMS films and the composite hydrogel, the tension sensing of the E-skin still functioned steadily after repeating tests (*SI Appendix*, Fig. S6 *A* and *B*).

To further explore the potential application values of the multifunctional E-skin, three pieces of red-colored E-skins were attached to three different fingers and the real-time signals of them under different stimuli were recorded. The E-skin affixed to the middle finger was utilized to detect signal changes during repeated contact with an ice bag (Fig. 5*A*). The pressure signals poked by a tweezer were recorded by the E-skin attached to the index finger. Besides, the tension signals detected by E-skin on thumb were generated by thumb bending. It was found that the colors of the materials changed significantly in the stimulated sites, including those that were touched with ice, poked by tweezers, and corresponded to the thumb joints. Therefore, the positioning of the stimulus site was successfully achieved on the

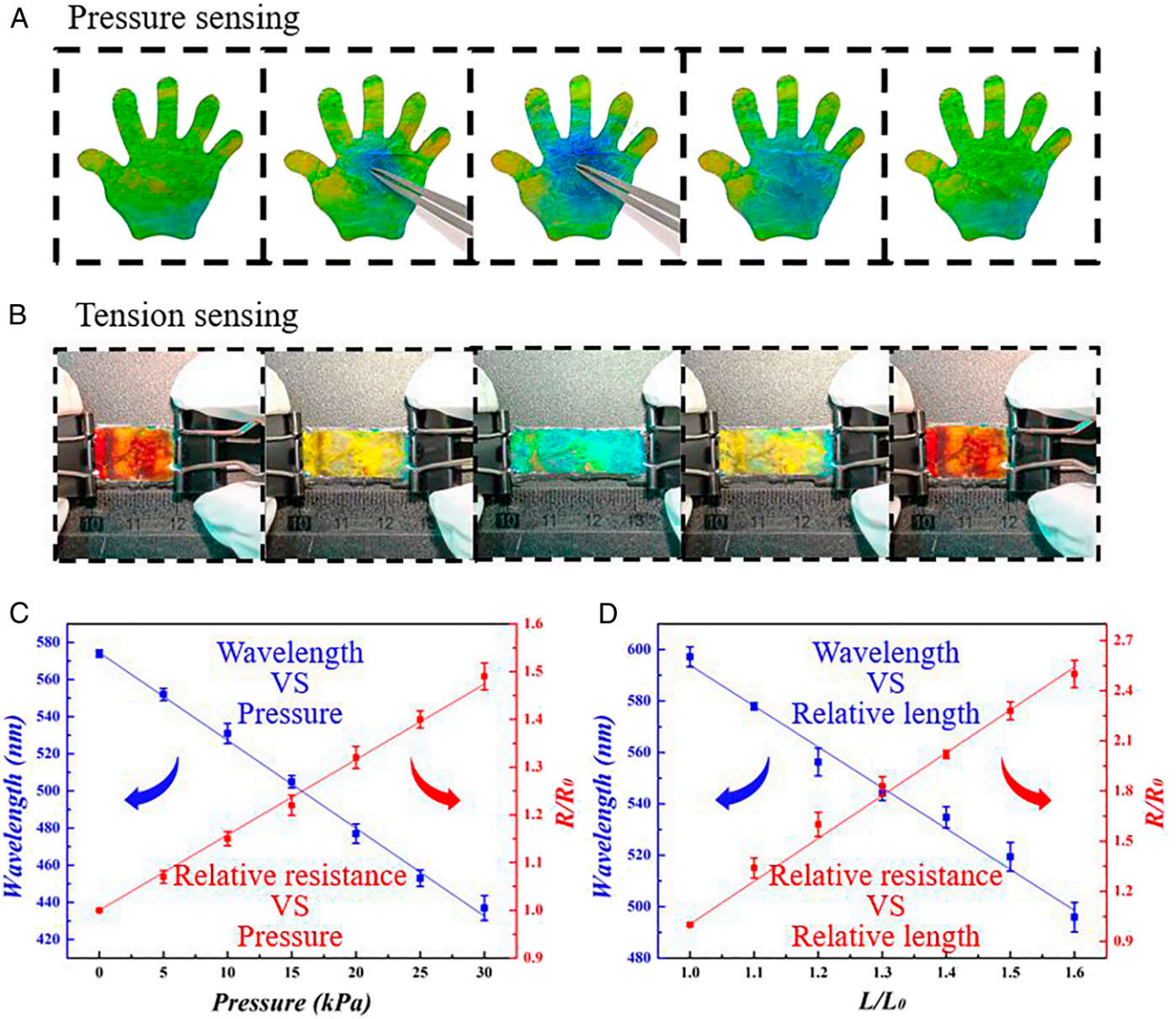

Fig. 4. The pressure and tension sensing test of the E-skin. (*A*) Optical images of the color variation of a palm-shaped E-skin under pressure. (*B*) Optical images of the color variation of a rectangular E-skin under tension. (*C*) The reflection peak wavelength and the relative resistance of the E-skin under different pressure. (*D*) The reflection peak wavelength and the relative resistance of the E-skin under stretching to different lengths.

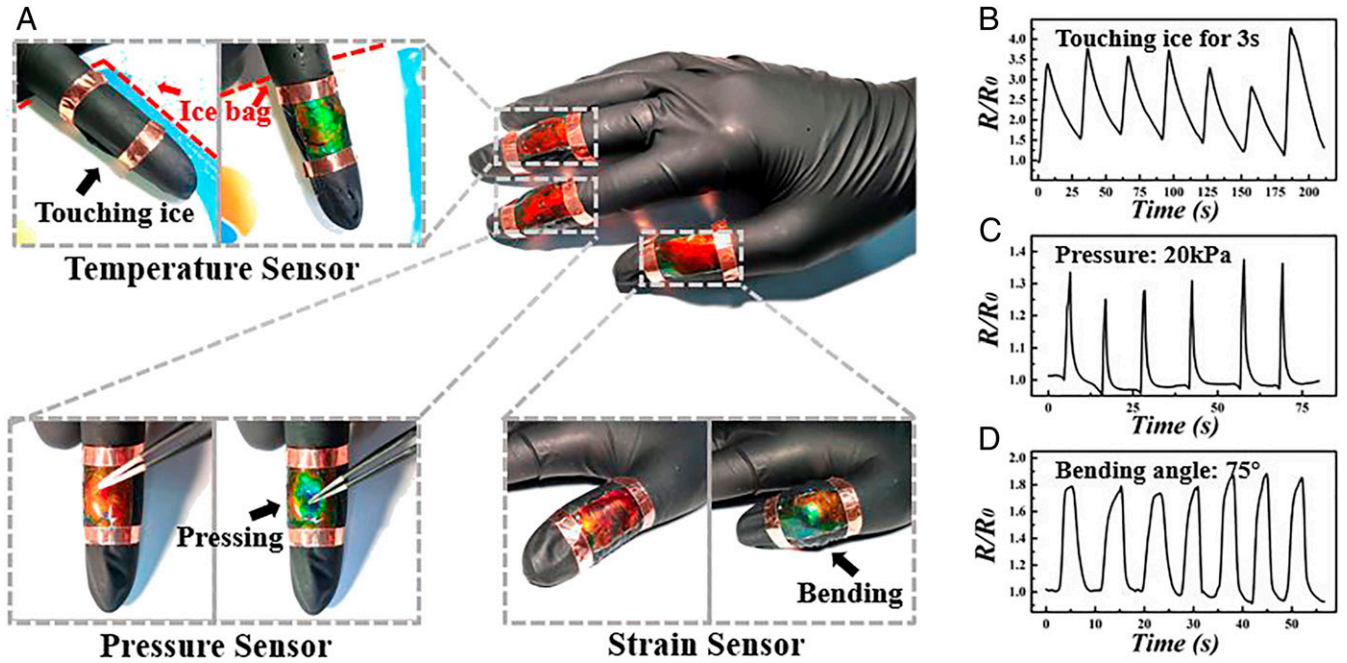

Fig. 5. The application of the multifunctional E-skins attached to human fingers. (*A*) Schematics and the optical images of the E-skins attached to human fingers. Three red-colored E-skins are affixed on different fingers and detect temperature, pressure, and tension, respectively. (*B–D*) The real-time signals of the variation of resistance of the E-skin under repeatedly (*B*) touching of ice for 3 s, (*C*) poking by tweezer with a pressure of 20 kPa, and (*D*) thumb bending with an angle of 75°.

visual interface through optical signals. In addition, the electrical signals recorded by the multimeter demonstrated that the resistances of the materials would vary accurately with the color-variation process, making it easy to quantify these stimuli (Fig. 5 *B*, *C* and *D*). In addition, when the form of the stimulus is unknown, the visual user-interaction interface provides a basis for signal recognition. It can be seen from the figure that when the color of the structural color hydrogel undergoes an overall change, the stimulation received by the E-skin is a change in ambient temperature. When the color of a certain area changes radioactively, it can be judged as a pressure stimulus, while when the overall color changes into a gradual color with directionality, the stimulus is tension. This example indicated that the multifunctional E-skin fabricated by conductive cellulose liquid-crystal hydrogels could provide an idea for the development of E-skin.

Discussion

Inspired by chameleons, we presented a multifunctional E-skin based on an HPC, PACA, and CNT composited conductive cellulose nanocrystal hydrogel. Due to the cholesteric liquid-crystal nanostructure of the HPC and the scaffold of intelligent responsive PACA hydrogel, the hydrogel was imparted with brilliant structural color and could optically report the changing of external stimuli such as temperature, pressure, and tension under the variation of internal nanostructures. Besides, the incorporation of CNT endowed the composite hydrogel with expected conductivity and the capability of reporting stimuli through resistance. These features indicated the E-skins fabricated by the composite hydrogel could not only quantitively feedback external stimulus through electrical resistance, but also map the stimulating sites by optical signals. Therefore, this dual-signal sensing ability made the conductive cellulose nanocrystal hydrogels expected to open a chapter in the design and the fabrication of multifunctional flexible E-skins.

Materials and Methods

Materials. HPC with a viscosity of 4.4 mPa·s (2% aqueous solution at 20 °C) was purchased from Nippon Soda Co., Ltd. Multiwalled CNTs dispersed solution (concentration: ~14 wt %, length: ~10 μm, diameter: ~50 nm) was bought from Nanjing XF NANO Materials Tech Co., Ltd. Acrylamide (AAm), acrylic acid (AAc), N,N′-methylenebisacrylamide (MBA), and 2-hydroxy-2-methylpropiophenone (HMPP) were purchased from Sigma-Aldrich. PDMS films with a thickness of 100 μm were purchased from Bald Advanced Materials Co., Ltd. The conductive tapes were bought from Meileqi Co., Ltd. Pure water (resistivity higher than 18 MΩ·cm) was acquired by a Milli-Q Plus 185 water purification system.

Preparation of the Conductive Cellulose Liquid-Crystal Hydrogel. The pregel solution of PACA was prepared first. When comprising a 10mL solution, we mixed 1g AAm (monomers), 1 g AAc (monomers), 0.1 g MBA (cross-linking agents), and 0.1 mL HMPP (photoinitiator) with deionized water. Before use, the pregel solution of PACA was stored at 4 °C without light. In order to generate the pregel solution of the composite hydrogel, HPC, CNTs, and the pregel solution of PACA with designated weight ratios were mixed in a lightproof mixer (Shengke Instruments). The dose of HPC and CNTs could be adjusted as needed for the desired color or conductivity. During this process, 50 mg HPC was added every 30 min, and the mixer continued to work for more than a week after everything was loaded. After extensive mixing, the solution was stirred every other week and was stored at 4 °C, away from light. To fabricate the conductive cellulose liquid-crystal hydrogel, the pregel solution was centrifuged (12 K rpm in 3–30 K, Sigma-Aldrich) for over 30 min for degassing. Then it was poured into the predesigned mold, kept for the self-assembly of cholesteric liquid crystal in the dark for about 10 min, and finally polymerized by UV light produced by a UV light-emitting diode (LED) curing system (OmniCure S1000). The polymerizing time should be over 30 min with a power density of 8,000 mW/cm^2. Thus, the composite conductive cellulose liquid-crystal hydrogel could be generated.

Fabrication of the Multifunctional E-Skin. First, a PDMS film was prepared as the substrate, and two conductive tapes were pasted on it with a certain distance. Two bar-shaped spacers were placed on the substrate. Then the pregel solution of the composite hydrogel was degassed and paved onto the substrate with a scraper, and then covered with another layer of PDMS. Thus, the E-skin was obtained by polymerizing the whole material under UV light for over 30 min. Finally, the spacers were removed and the cured material was cut into the desired shape. The thickness of the hydrogel could be adjusted by alternating the height of the spacers. In Figs. 4 and 5, the palm-shaped E-skin was about 2.5 cm × 2.5 cm × 0.4 cm. The size of the

E-skin for the tension test is about 2 cm × 1.5 cm × 0.4 cm. In Fig. 5, the sizes of the E-skins pasted on fingers were also 2 cm × 1.5 cm × 0.4 cm.

The Heating, Pressure, and Tension Tests of the Dual-Signal E-Skin. For the heating test, the material was heated on an electrical heater (Dragon Lab MS-H-Pro). For the pressure end tension experiment, the pressure and tension were provided by a spring tension/pressure tester (Shigan Instrument). The variations of the E-skins were captured by a single lens reflex camera.

Characteristics of the Materials. The variations of the reflection peak of the dual-signal E-skin were recorded by a fiberoptic spectrometer (Ocean Optics; USB2000-FLG) equipped on an optical microscope (Olympus BX51). The resistances of the materials were measured with a traditional two-probe technique by a semiconductor characterization system (4200-SCS, Keithley).

The pressure and tension on E-skins were measured by a multifunctional mechanical measuring instrument (Shanghai Henggang Instrument). The real-time resistance changes of the dual-signal E-skin were recorded by a digital multimeter (Keithley).

Data Availability. All data are contained in the manuscript text and *SI Appendix*.

ACKNOWLEDGMENTS. This work was supported by the National Natural Science Foundation of China (Grants 61927805 and 51522302), the National Natural Science Foundation of China (Grant U1530260), the National Science Foundation of Jiangsu (Grant BE2018707), the Postdoctoral Science Foundation of China (Grant 2019 M653061), and the Scientific Research Foundation of Southeast University.

1. J. C. Yang *et al*., Electronic skin: Recent progress and future prospects for skin-attachable devices for health monitoring, robotics, and prosthetics. *Adv. Mater.* **31**, e1904765 (2019).
2. J. Y. Oh, Z. Bao, Second skin enabled by advanced electronics. *Adv. Sci. (Weinh.)* **6**, 1900186 (2019).
3. C. M. Boutry *et al*., Biodegradable and flexible arterial-pulse sensor for the wireless monitoring of blood flow. *Nat. Biomed. Eng.* **3**, 47–57 (2019).
4. D. Son, Z. Bao, Nanomaterials in skin-inspired electronics: Toward soft and robust skin-like electronic nanosystems. *ACS Nano* **12**, 11731–11739 (2018).
5. Y. Yu, J. Guo, L. Sun, X. Zhang, Y. Zhao, Microfluidic generation of microsprings with ionic liquid encapsulation for flexible electronics. *Research (Wash D C)* **2019**, 6906275 (2019).
6. J. Xu *et al*., Multi-scale ordering in highly stretchable polymer semiconducting films. *Nat. Mater.* **18**, 594–601 (2019).
7. H. Xia, Y. Ran, H. Li, X. Tao, D. Wang, Freestanding monolayered nanoporous gold films with high electrocatalytic activity via interfacial self-assembly and overgrowth. *J. Mater. Chem. A* **1**, 4678–4684 (2013).
8. S. R. Shin *et al*., Graphene-based materials for tissue engineering. *Adv. Drug Deliv. Rev.* **105**, 255–274 (2016).
9. Y. Liu *et al*., Soft and elastic hydrogel-based microelectronics for localized low-voltage neuromodulation. *Nat. Biomed. Eng.* **3**, 58–68 (2019).
10. I. Bita *et al*., Graphoepitaxy of self-assembled block copolymers on two-dimensional periodic patterned templates. *Science* **321**, 939–943 (2008).
11. J. Sun *et al*., Composite films with ordered carbon nanotubes and cellulose nanocrystals. *J. Phys. Chem. C* **121**, 8976–8981 (2017).
12. M. Liao *et al*., Wearable, healable, and adhesive epidermal sensors assembled from mussel-inspired conductive hybrid hydrogel framework. *Adv. Funct. Mater.* **27**, 1703852 (2017).
13. G. Cai *et al*., Extremely stretchable strain sensors based on conductive self-healing dynamic cross-links hydrogels for human-motion detection. *Adv. Sci. (Weinh.)* **4**, 1600190 (2016).
14. P. V. Braun, Materials science: Colour without colourants. *Nature* **472**, 423–424 (2011).
15. G. H. Lee *et al*., Colloidal photonic inks for mechanochromic films and patterns with structural colors of high saturation. *Chem. Mater.* **31**, 8154–8162 (2019).
16. C. G. Schaefer *et al*., Reversible light-, thermo-, and mechano-responsive elastomeric polymer opal films. *Chem. Mater.* **25**, 2309–2318 (2013).
17. H.-H. Chou *et al*., A chameleon-inspired stretchable electronic skin with interactive colour changing controlled by tactile sensing. *Nat. Commun.* **6**, 8011 (2015).
18. M. Kolle *et al*., Mimicking the colourful wing scale structure of the Papilio blumei butterfly. *Nat. Nanotechnol.* **5**, 511–515 (2010).
19. S. K. Smoukov, S. Gangwal, M. Marquez, O. D. Velev, Reconfigurable responsive structures assembled from magnetic Janus particles. *Soft Matter* **5**, 1285–1292 (2009).
20. D. Ge *et al*., A robust smart window: Reversibly switching from high transparency to angle-independent structural color display. *Adv. Mater.* **27**, 2489–2495 (2015).
21. Y. Huang *et al*., Colloidal photonic crystals with narrow stopbands assembled from low-adhesive superhydrophobic substrates. *J. Am. Chem. Soc.* **134**, 17053–17058 (2012).
22. K. R. Phillips *et al*., A colloidoscope of colloid-based porous materials and their uses. *Chem. Soc. Rev.* **45**, 281–322 (2016).
23. Z. Mao, H. Xu, D. Wang, Molecular mimetic self-assembly of colloidal particles. *Adv. Funct. Mater.* **20**, 1053–1074 (2010).
24. L. Wu *et al*., Printing patterned fine 3D structures by manipulating the three phase contact line. *Adv. Funct. Mater.* **25**, 2237–2242 (2015).
25. L. Wang *et al*., Inkjet printed colloidal photonic crystal microdot with fast response induced by hydrophobic transition of poly(N-isopropyl acrylamide). *J. Mater. Chem.* **22**, 21405–21411 (2012).
26. H. Yi *et al*., Ultra-adaptable and wearable photonic skin based on a shape-memory, responsive cellulose derivative. *Adv. Funct. Mater.* **29**, 1902720 (2019).
27. J. Ge, Y. Yin, Responsive photonic crystals. *Angew. Chem. Int. Ed. Engl.* **50**, 1492–1522 (2011).
28. Y. S. Zhang, A. Khademhosseini, Advances in engineering hydrogels. *Science* **356**, eaaf3627 (2017).
29. H. Kim *et al*., Structural colour printing using a magnetically tunable and lithographically fixable photonic crystal. *Nat. Photonics* **3**, 534–540 (2009).
30. J. Hou *et al*., Bio-inspired photonic-crystal microchip for fluorescent ultratrace detection. *Angew. Chem. Int. Ed. Engl.* **53**, 5791–5795 (2014).
31. S. Kim *et al*., Silk inverse opals. *Nat. Photonics* **6**, 817–822 (2012).
32. F. Fu, L. Shang, Z. Chen, Y. Yu, Y. Zhao, Bioinspired living structural color hydrogels. *Sci. Robot.* **3**, eaar8580 (2018).
33. F. Fu *et al*., Bio-inspired self-healing structural color hydrogel. *Proc. Natl. Acad. Sci. U.S.A.* **114**, 5900–5905 (2017).
34. Y. Yue *et al*., Mechano-actuated ultrafast full-colour switching in layered photonic hydrogels. *Nat. Commun.* **5**, 4659 (2014).
35. H. Kang, J.-S. Lee, W. S. Chang, S.-H. Kim, Liquid-impermeable inverse opals with invariant photonic bandgap. *Adv. Mater.* **27**, 1282–1287 (2015).
36. Y. Heo, H. Kang, J.-S. Lee, Y.-K. Oh, S.-H. Kim, Lithographically encrypted inverse opals for anti-counterfeiting applications. *Small* **12**, 3819–3826 (2016).
37. Z. Zhang, Z. Chen, L. Sun, X. Zhang, Y. Zhao, Bio-inspired angle-independent structural color films with anisotropic colloidal crystal array domains. *Nano Res.* **12**, 1579–1584 (2019).
38. Z. Zhang *et al*., Bioinspired bilayer structural color hydrogel actuator with multi-environment responsiveness and survivability. *Small Methods* **3**, 1900519 (2019).
39. C. Shao *et al*., Responsive inverse opal scaffolds with biomimetic enrichment capability for cell culture. *Research (Wash D C)* **2019**, 9783793 (2019).
40. R. S. Werbowyj, D. G. Gray, Liquid-crystalline structure in aqueous hydroxypropyl cellulose solutions. *Mol. Cryst. Liq. Cryst. (Phila. Pa.)* **34**, 97–103 (1976).
41. G. Kamita *et al*., Biocompatible and sustainable optical strain sensors for large-area applications. *Adv. Opt. Mater.* **4**, 1950–1954 (2016).
42. H.-L. Liang *et al*., Roll-to-roll fabrication of touch-responsive cellulose photonic laminates. *Nat. Commun.* **9**, 4632 (2018).
43. J. Zheng *et al*., Mimosa inspired bilayer hydrogel actuator functioning in multi-environments. *J. Mater. Chem. C* **6**, 1320–1327 (2018).
44. J. Dong, J. Ding, J. Weng, L. Dai, Graphene enhances the shape memory of poly (acrylamide-co-acrylic acid) grafted on graphene. *Macromol. Rapid Commun.* **34**, 659–664 (2013).
45. T. Li *et al*., Synthesis and Water Absorbency of Poly(acrylic acid-co-acrylamide). *Adv. Mater. Research* **250–253**, 695–698 (2011).
46. H. Devries, Rotatory power and other optical properties of certain liquid crystals. *Acta Crystallogr.* **4**, 219–226 (1951).